
New production stimulated by high-frequency winds in a turbulent mesoscale eddy field

M. Lévy^{1,*}, P. Klein², and M. Ben Jelloul²

¹ LOCEAN, IPSL, Université Pierre et Marie Curie, CNRS, Paris, France

² LPO, IFREMER, UBO, CNRS, Brest, France

*: Corresponding author : M. Lévy, email address : Marina.Levy@locean-ipsl.upmc.fr

Abstract:

Using an idealized model of an oligotrophic open-ocean region characterized by intense sub-mesoscale turbulence, we show that the presence of energetic near-inertial motions, forced by high-frequency winds, triggers transient nutrient inputs in the surface mixed-layer, stimulating new production. We also show that this production increase is larger than the increase due to the Ekman transport resulting from a slow-evolving wind forcing. The nutrient supplies are due to the interaction between near-inertial motions and the sub-mesoscale frontogenetic dynamics that reinforces both the vertical advection and vertical diffusion, especially within sub-mesoscales features. The net result is an uplift of new production from the subsurface to the mixed-layer. A direct consequence is that the sub-mesoscale filamentary patterns of phytoplankton should become much more observable from space in the presence of high-frequency winds.

1. Introduction

16 In offshore oligotrophic regions the intensity of new production (NP) is strongly related
17 to the vertical nutrient transport, and in particular to that associated with mesoscale
18 eddies (with diameter $O(100\text{km})$) (McGillicuddy et al., 1998). Recently the focus has
19 shifted to submesoscales ($O(1-10\text{km})$) that are ubiquitous in a turbulent eddy field. In-
20 deed theoretical and high resolution numerical studies (Capet et al., 2008, Klein et al.,
21 2008) indicate that vertical exchanges of tracers in the upper oceanic layers mostly occur
22 at small-scale and preferentially within submesoscales located around or outside mesoscale
23 eddies. The main physics is the surface frontogenesis that triggers intense vertical veloc-
24 ities within these submesoscales. Results of Levy et al. (2001) (hereafter LKT), who
25 examined the transient response of an oligotrophic production regime in a mesoscale eddy
26 field, further highlight the biogeochemical impact of these submesoscales. They showed
27 that NP is greatly enhanced by the vertical injection of nutrients occurring within sub-
28 mesoscale structures, in particular anticyclonic filaments. High-resolution observations of
29 biogeochemical parameters (Niewiadomska et al., 2008; Jonhson et al., 2008), that reveal
30 the existence of very thin tongues of tracer in regions of strong density fronts, support
31 this vision of such submesoscale impacts.

32 Presence of a non-zero wind forcing further affects the vertical nutrient injection driven
33 by submesoscales. The wind forcing considered (such as daily-averaged winds) usually
34 includes only its low-frequency (LF) component (with respect to the Coriolis frequency
35 f). Resulting effects are nonlinear Ekman pumping and eventually front intensification at
36 the submesoscale edges (Thomas and Lee, 2005; Mahadevan et al., 2008). High-frequency

37 (HF) winds (such as those present in 3-hourly realistic wind time series), that are known
38 to efficiently force near-inertial motions, may trigger a much larger nutrient uplift (Klein
39 and Coste, 1984). Furthermore, in presence of a mesoscale turbulent field, such HF winds
40 bring into play new physics: these structures efficiently polarize near-inertial motions,
41 trapping them in small-scale anticyclonic structures (Young and Ben Jelloul, 1997; Klein
42 et al., 2004). Impacts of these HF winds on the resulting submesoscale vertical advection
43 and diffusion should further affect the vertical exchanges of tracers, which still needs to
44 be investigated in particular in terms of the consequences on the biogeochemical system.

45 Thus the question addressed in the present study is: does the interaction of HF winds
46 with a turbulent eddy field affects the oligotrophic NP through its impacts on the vertical
47 mixing and the vertical velocity field? For that purpose, the numerical experiments of
48 LKT are repeated but including HF winds (with frequencies spanning around f). More
49 precisely our approach is to isolate the impact of near-inertial waves from the impact of
50 Ekman fluxes. This is done by comparing simulations forced with winds with frequencies
51 close to f , where both effects are present, with simulations forced with constant winds,
52 where the near-inertial oscillations are much reduced and thus where the impact of Ekman
53 fluxes prevails.

2. Numerical experiments

54 Following LKT, a high-resolution primitive equation model coupled with an ecosys-
55 tem model (NO₃-NH₄-P-Z-D-DOM) is used to simulate primary productivity in an olig-
56 otrophic region characterized by intense mesoscale activity, during the stratified season.
57 Vertical diffusion is calculated with a 1.5 turbulent closure model (Blanke and Delecluse,

1993). Other details of the model are given in LKT. The initial conditions are constructed as follows. Interactive mesoscale vortices with submesoscale vorticity filaments between and around them (Fig. 1a,b,e) are generated from the spin-down of a large-scale unstable zonal jet, in a periodic β -plane channel centered at 30°N ($f = 8 \times 10^{-5}\text{s}^{-1}$). The initial conditions for the ecosystem are homogeneously set from the steady state solution away from the interacting vortices. They are representative of a highly oligotrophic system, typical of summer conditions at mid latitudes; the nitracline and NP subsurface maxima are located at 120 m depth and the mixed-layer is shallow ($\approx 40\text{m}$) (Fig. 1f,g). The absence of a large scale horizontal nutrient gradient enables us to highlight the vertical processes: any additional vertical transport of nutrient into the euphotic layer destabilizes the biological steady state by stimulating new production (LKT). Sub-mesoscale fronts associated with the filaments trigger intense vertical velocities, which leads to significant nutrient injection and NP. NP is confined within the vorticity filaments, where both vertical velocities and horizontal stretching are strong (Fig. 1d). The nutricline and the subsurface NP maximum are closer to the surface ($\approx 60\text{m}$) in regions of strong upwelling (Fig. 1f,g).

We present the results of four experiments varying in wind forcings (Table 1). The experiments are performed during 10 days, starting from the initial conditions shown in Fig. 1. During these 10 days, the mesoscale eddy field slowly evolves, with, in particular, the deformation and westward propagation of the main vortices over 20-40 km (not shown). The wind forcing is homogeneous and eastward, thus with no preferred angle with respect to the submesoscale fronts which are oriented in all directions. The wind is

80 constant ($0.1Nm^{-2}$) in the CW experiment. The wind is time-varying with inertial (f)
81 and subinertial ($0.75f$) frequencies in IW and SW (square oscillatory functions varying
82 between 0 and $0.2Nm^{-2}$, thus with $0.1Nm^{-2}$ mean). In NW, the integration is simply
83 continued with no wind.

3. Results

84 We examine the differences in NP that result from the different wind scenarios. NP is
85 computed as the consumption of nitrate by phytoplankton for photosynthesis and is ver-
86 tically integrated, either over the euphotic layer (0-150m, NP_{tot}) or closer to the surface
87 (0-50m, NP_{surf}). Results are summarized in Table 1. A non-zero wind forcing system-
88 atically increases NP. The NP increase is much stronger when the wind is variable in
89 time and, this increase is particularly strong in the surface mixed-layer. More precisely
90 in the constant wind experiment, NP_{tot} is almost unchanged with respect to the no wind
91 experiment (+2%). In the case of variable winds, a moderate increase is obtained for
92 sub-inertial winds (+10%) and a larger one for inertial winds (+20%). NP_{surf} increases
93 by +55% with a constant wind and +233% with an inertial wind (Table 1).

94 We now examine the processes responsible for the mean increase of NP_{tot} . Table 1
95 shows the mean vertical fluxes (advective and diffusive) of nitrate across 150m for all ex-
96 periments. Diffusive fluxes are two orders of magnitude smaller than the advective fluxes,
97 clearly suggesting that the NP_{tot} increase results from an increase of the advective supply
98 of nitrate at the base of the euphotic layer. The advective supply of nitrate is maximum
99 in the inertial wind experiment, intermediate in the subinertial wind experiment, and
100 minimum in the no wind and constant wind experiments.

101 The 0-50m nutrient budget is also dominated by the advective supply of nitrate (Ta-
102 ble 1). However, vertical diffusion becomes non-negligible since, with inertial and subin-
103 ertial winds, it represents, at 50m, about one third of the total nitrate supplies. This is due
104 to the deepening of the mixed-layer below 50m with HF winds (Fig. 2 b). Furthermore,
105 vertical diffusion takes over vertical advection. Indeed, with HF winds, the intensified
106 vertical advection is able to move subsurface maxima of NP and phytoplankton, and also
107 the deeper nutricline, closer to the surface. This the case within the submesoscale struc-
108 tures affected by frontogenesis (Fig. 2). Then vertical diffusion brings the biogeochemical
109 material to the surface mixed-layer (Fig. 2).

110 The uplift of nutrient from subsurface to the surface strongly reduces the time scale of
111 the biological response to nutrient supplies which further increases NP. This is because at
112 sub-surface the lack of light is a strong limiting factor of productivity. To quantify this
113 effect, we estimate the phytoplankton effective growth rate $\mu = NP/PHY$ (in d^{-1}), where
114 NP is new production (in $mmoleN\ m^{-3}d^{-1}$) and PHY is the concentration of phytoplank-
115 ton (in $mmoleN\ m^{-3}$). In all experiments, the time scale associated with phytoplankton
116 growth, $1/\mu$, is close to 10 days when NP occurs at 100m, and can be as fast as 1 day when
117 NP occurs at 10m. Thus, close to the surface, the biological response time scale becomes
118 close to the inertial frequency, which enables the partial utilization of the nutrients that
119 are advected by the near-inertial waves. This is supported by the nutrient budgets: the 0-
120 150m nutrient supplies are not immediately uptaken by NP ($0-150m\ (AD + DF) > NP_{tot}$
121 in Table 1), while the 0-50m supplies equal NP ($0-50m\ (AD + DF) \approx NP_{surf}$ in Table

122 1). These dynamical and biological arguments explain the much stronger change in the
123 surface mixed-layer (NP_{surf}) compared to the change in total NP (NP_{tot}).

4. Discussion

124 The additional NP uplift with HF winds thus results both from the stronger vertical
125 advection at 50m and from the stronger diffusion (Table 1). We discuss how HF winds
126 may affect these physical mechanisms.

127 Impacts of HF winds on vertical velocity (W) is illustrated on Fig. 3, which shows the
128 time evolution of W and NP across a filament oriented approximately along the NW-SE
129 direction (see Fig. 1). In the no wind experiment, W has a bipolar structure characteristic
130 of frontogenesis (Hoskins and Bretherton, 1972), with upwelling (downwelling) on the
131 warm (cold) side of the filament (Fig. 3a). It varies between $-20/+10$ m/day. With
132 HF winds, W shows distinct near-inertial oscillations (Fig. 3b). and varies between -
133 $81/+47$ md^{-1} . Most of all, there is a clear asymmetry in the upwelling/downwelling
134 motions associated to the near-inertial motions leading to a dominance of upwellings
135 (downwellings) on the warm (cold) side of the front (Fig. 3b). Averaged over an inertial
136 period, the mean W -fields (not shown) from the HF wind experiments emphasize the
137 impact of this asymmetry, displaying the same positive and negative patterns as Fig. 3a
138 but with larger amplitude and spatial extension. Thus contribution of the near-inertial
139 motions appears to reinforce the contribution of the vertical velocity associated with
140 the frontogenesis. The W -frequency spectra of Fig. 3c confirm the preceding results,
141 concerning not only the strong energy increase at the inertial frequency but also the
142 significant increase at lower frequencies. Increase of the mean vertical velocity in presence

143 of HF winds has been observed as well in high-resolution numerical simulations of a fully
144 turbulent mesoscale eddy field (Klein et al., in preparation) and appears to be due to
145 the nonlinear interactions between near-inertial waves as already noticed in Klein and
146 Treguier (1993). Understanding these characteristics requires a more thorough dynamical
147 study that is beyond the scope of the present study, but that would extend the results of
148 Thomas and Lee (2005).

149 Regarding diffusion, HF winds are known to increase the amplitude of the diffusion
150 fluxes and to deepen the mixed-layer (Klein and Coste, 1984). This is due to the energetic
151 near-inertial motions that produce strong vertical shears at the mixed-layer base. But this
152 mixed-layer deepening and diffusion fluxes are also modulated by the submesoscales. As
153 mentioned in the introduction, energetic near-inertial motions become rapidly trapped
154 within submesoscales and principally within anticyclonic structures. This means that dif-
155 fusion fluxes and mixed-layer deepening are enhanced in those regions where furthermore
156 the vertical velocity is statistically upward. Both mechanisms act consequently in phase
157 to further uplift biogeochemical material in the surface layers.

158 These stronger vertical velocity and diffusion is accompanied by an intensification of
159 NP_{tot} as illustrated by the comparison of Fig. 3 d and e. The NP spectrum (Fig. 3f), on
160 the other side, shows that the increase of NP in response to HF winds NP mostly concerns
161 the low-frequency part of the spectrum (although there is a signal close to the wind forcing
162 frequency). This reflects the cumulative uptake of nutrients by phytoplankton that acts
163 as a time-integrator of the advective fluxes.

5. Conclusion

164 Our results suggest that HF winds re-inforce vertical velocities, as well as the mixed-
165 layer deepening, within submesoscale structures. These effects stimulate NP, particularly
166 close to the surface, with a smaller impact on the total NP budget. A direct consequence
167 is that the submesoscale filamentary patterns of phytoplankton become observable from
168 space in the presence of HF winds, which is not the case without wind (see Fig. 2c and d).
169 By comparing experiments with the same time-mean wind stress but with different wind
170 frequencies, we have shown that the increase of NP due to near-inertial oscillations is more
171 important than the increase due to the Ekman transport resulting from a slow-evolving
172 wind forcing.

173 The present results are based on transient, highly idealized model simulations, and are
174 not quantitatively representative of any specific biogeochemical provinces. In particular,
175 the intensity of the vertical transport depends on many parameters such as the nutrient
176 large-scale field and the strength of the mesoscale eddy field. Estimating their contribution
177 to basin-scale budgets requires long simulations at the scale of an ocean basin, which will
178 involve complex adjustments associated with the equilibration of the circulation and of
179 the nutrient pool. However the present results suggest that a complete understanding of
180 submesoscale-biological interactions needs also to take into account the interaction with
181 rapid phenomenon such as near-inertial waves forced by HF winds.

182 **Acknowledgments.** The calculations reported in this study were performed on the
183 NEC SX8 of IDRIS (France). The authors thank Xavier Capet for his useful comments
184 and Leif Thomas for encouraging us to publish these results.

References

- 185 Blanke, B. and P. Delecluse, Variability of the tropical Atlantic Ocean simulated by a
186 general circulation model with two different mixed-layer physics, *J. Phys. Oceanogr.*,
187 *23*, 1363-1388, 1993.
- 188 Capet, X., J. C. McWilliams, M.J. Molemaker and A.F. Shchepetkin, Mesoscale to Sub-
189 mesoscale transition in the California Current System. Part 2: Dynamical Processes
190 and Observational Tests, *J. Phys. Oceanogr.*, *38*, 44-64, 2008.
- 191 Hoskins, B.J. and F.P. Bretherton, Atmospheric frontogenesis models : mathematical
192 formulation and solution, *J. Atmos. Sciences*, *29*, 11-37, 1972.
- 193 Johnson, K S, Coletti, L , Jannasch, H , Martz, T , Swift, D and Riser, S: Long-Term Ob-
194 servations of Ocean Biogeochemistry with Nitrate and Oxygen Sensors in Apex Profiling
195 Floats, *Eos Trans. AGU*, *89*(53), Fall Meet. Suppl., Abstract OS31A-1232, 2008.
- 196 Klein, P. and B. Coste, Effects of wind-stress variability on nutrient transport into the
197 mixed layer, *Deep-Sea Res.*, *31*, 21-37, 1984.
- 198 Klein, P. and A.M. Tréguier, 1993. Inertial resonances induced by a geostrophic jet. *J.*
199 *Phys. Oceanogr.*, *23*, 1897-1915.
- 200 Klein, P., Hua B.L., G. Lapeyre, X. Capet, S. LeGentil and H. Sasaki., Upper Ocean
201 Dynamics from High 3-D Resolution Simulations, *J. Phys. Ocean.*, *38*, 1748-1763, 2008.
- 202 Klein, P., W. Large and G. Lapeyre, Wind ringing of the ocean in presence of mesoscale
203 eddies, *Geophys. Res. Let.*, *31*, L15306, doi:10.1029/2004GL020274, 2004.
- 204 Levy, M., P. Klein and A. M. Treguier: Impacts of sub-mesoscale physics on phytoplankton
205 production and subduction, *J. Mar. Res.*, *59*, 535-565, 2001.

- 206 Mahadevan, A., L. Thomas, and A. Tandon, Comment on Eddy/Wind Interactions Stim-
207 ulate Extraordinary Mid-Ocean Plankton Blooms. *Science*, 320(5875), 2008.
- 208 McGillicuddy, D. J. Jr., A. R. Robinson, D. A. Siegel, H. W. Jannasch, R. Johnson, T.
209 D. Dickey, J. McNeil, A. F. Michaels and A. H. Knap: Influence of mesoscale eddies on
210 new production in the Sargasso Sea, *Nature*, **394**, 263, 1998.
- 211 Niewiadomska, K., H. Claustre, L. Prieur and F. d'Ortenzio, Submesoscale physical-
212 biogeochemical coupling across the Ligurian Current (northwestern Mediterranean) us-
213 ing a bio-optical glider, *Limnol. Ocean.*, 53, 2210-2225, 2008.
- 214 Thomas, L. N., and C. M. Lee, Intensification of ocean fronts by down-front winds, *J.*
215 *Phys. Oceanogr.*, 35, 1086-1102, 2005.
- 216 Young, W. R. and Ben Jelloul, M., Propagation of Near Inertial Oscillations through a
217 Geostrophic Flow, *J. Mar. Res.*, 55, 735-766, 1997.

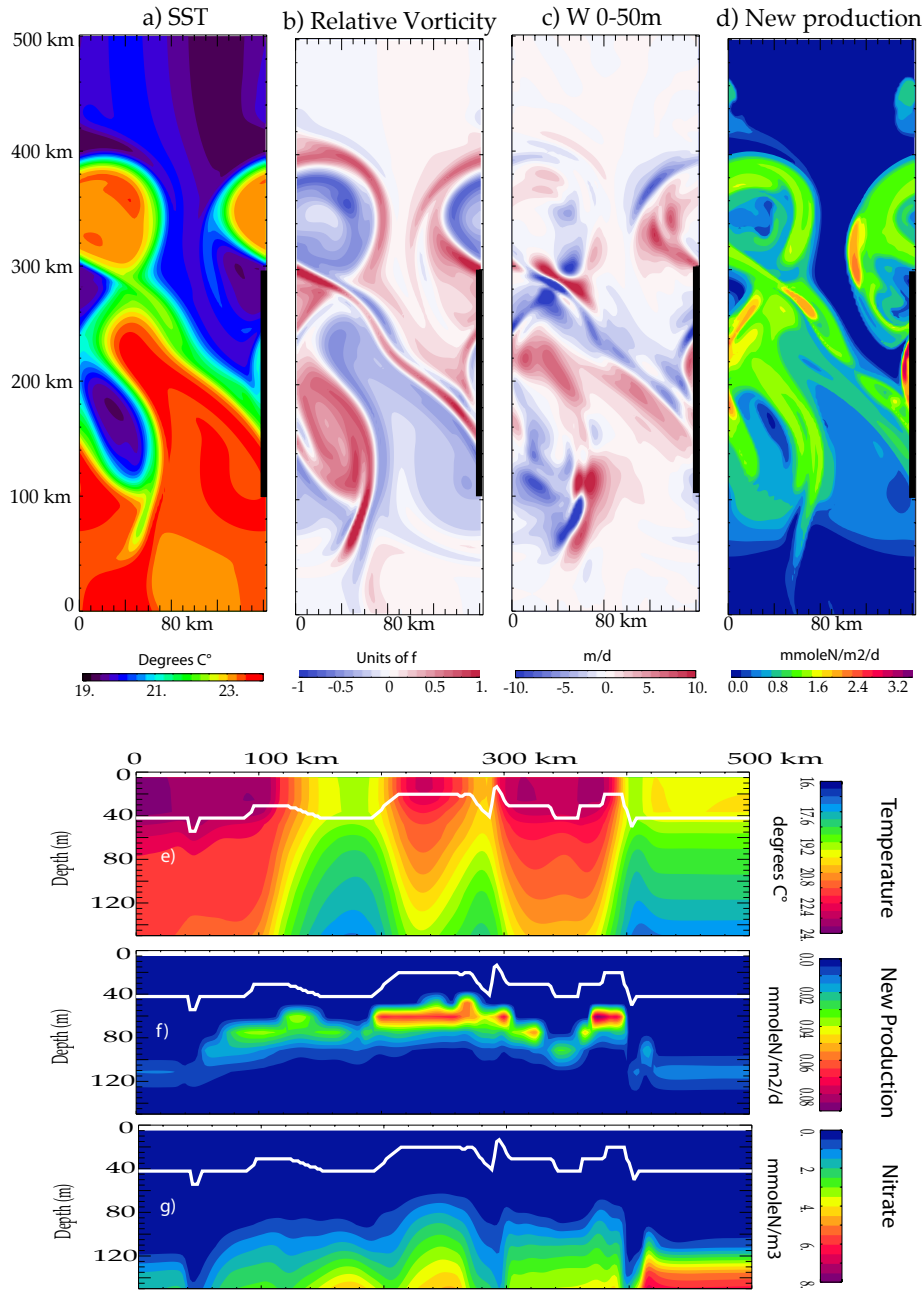


Figure 1. Model fields before the wind forcing is applied. Panels a), b), c) and d): horizontal views of sea surface temperature (SST), relative vorticity at the surface, vertical velocity averaged from 0-50 meters and new production integrated between 0-150 meters. Panels e), f) and g): vertical section along $x=30$ km of temperature, new production and nitrate. The thick vertical black line on panels a), b), c) and d) marks the position of the latitudinal section shown in Fig.

3. The white line on panels e), f) and g) is the mixed-layer depth.

D R A F T

July 8, 2009, 12:02pm

D R A F T

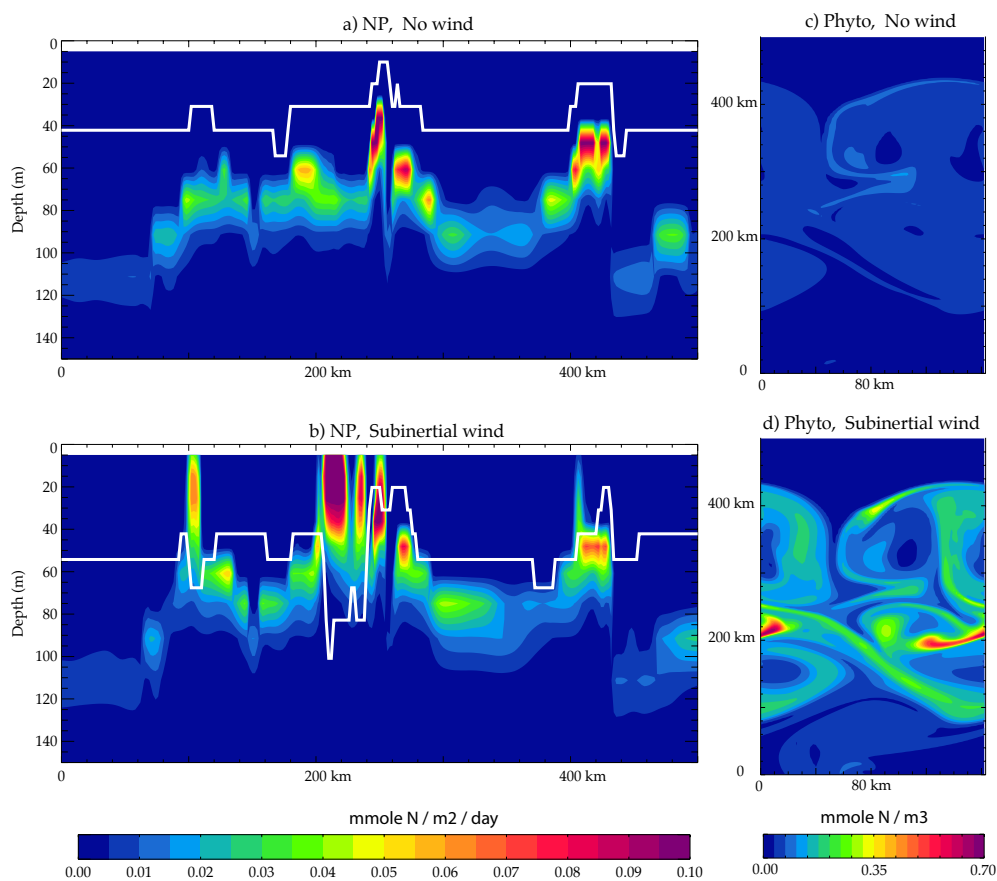


Figure 2. Vertical section of new production after 10 days along $x=0$ km in the experiments with no wind (panel a) and with sub-inertial wind (panel b); the white line shows the mixed-layer depth. Panels c and d show the corresponding imprint on sea-surface phytoplankton.

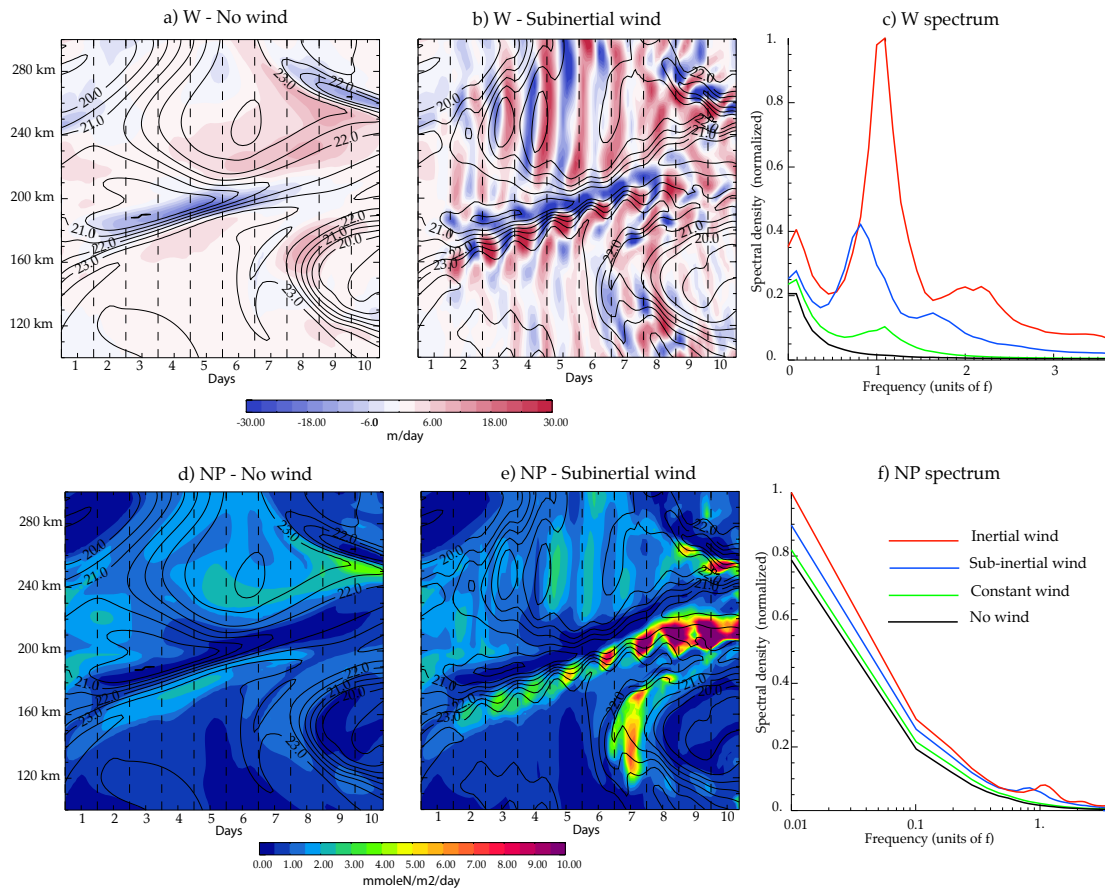


Figure 3. Hovmoller of the 0-50m vertical velocity along $x=180$ km in the experiment with no wind (panel a) and with subinertial wind (panel b); contours show the sea surface temperature. The position of the section is shown by the thick vertical black line on the right side of the top panels in Fig. 1. c) Frequency spectrum of 0-50m vertical velocity in the four experiments. d), e) and f): Same as a), b) and c) but for the 0-150m new production. Note that a log scale is used along the x-axis in panel f and a linear scale in panel c.

Table 1. Wind forcing and mean nutrient budgets for the four model experiments: no wind (NW), constant wind (CW), subinertial wind (SW) and inertial wind (IW). The new production (NP), advection (AD) and vertical diffusion (DF) budgets are expressed in mmoleN/m²/d. They are averaged over the 10 days of the experiments and over the entire model domain. Fluxes are integrated over different vertical layers: 0-150m and 0-50m. Percentages indicated in brackets refer to the percent increase with respect to the NW experiment.

	NW	CW	SW	IW
mean wind stress (Nm^{-2})	0	0.1	0.1	0.1
wind stress frequency	-	-	0.75 f	f
wind stress period (h)	-	-	25.1	18.8
0-150m NP	0.82	0.84 (+2%)	0.90 (+10%)	0.98 (+20%)
0-150m AD	1.03	1.00	1.08	1.22
0-150m DF	0.04	0.04	0.04	0.04
0-50m NP	0.09	0.14 (+55%)	0.23 (+155%)	0.30 (+233%)
0-50m AD	0.11	0.14	0.20	0.23
0-50m DF	0.005	0.03	0.08	0.11